

Bottom Tetraquark Production at RHIC?

R. Vogt

*Nuclear and Chemical Sciences Division, Lawrence Livermore National Laboratory, Livermore, CA 94551, USA and
Department of Physics and Astronomy, University of California, Davis, CA 95616, USA*

A. Angerami

Nuclear and Chemical Sciences Division, Lawrence Livermore National Laboratory, Livermore, CA 94551, USA

Background: A resonance has been observed by the ANDY Collaboration at the Relativistic Heavy-Ion Collider at Brookhaven National Laboratory in Cu+Au collisions at center-of-mass energy $\sqrt{s} = 200$ GeV and at forward rapidity with an average mass of 18.15 GeV. The Collaboration suggests that it is a $b\bar{b}b\bar{b}$ tetraquark state decaying to two $\Upsilon(1S)$ states, each measured through the $\Upsilon \rightarrow ggg$ channel. **Purpose:** Their suggestion is investigated assuming that the two Υ states are produced through the materialization of a $|uud\bar{b}\bar{b}\bar{b}\bar{b}\rangle$ Fock state in the projectile. **Methods:** The Υ pair mass and rapidity distributions arising from such a state are calculated. The production of an $X_b(b\bar{b}b\bar{b})$ tetraquark state from the same Fock configuration is also investigated. The dependence on bottom quark mass and their transverse momentum range is also studied. **Results:** It is found that double Υ production from these $|uud\bar{b}\bar{b}\bar{b}\bar{b}\rangle$ states peak in the rapidity range of the ANDY detector. The Υ pair and X_b masses are, however, higher than the mass reported by the ANDY Collaboration. **Conclusions:** The results obtained from these calculations are incompatible with the ANDY result. They are, however, compatible with previous predictions of $b\bar{b}b\bar{b}$ tetraquark masses.

I. INTRODUCTION

Quantum Chromodynamics (QCD) is the theory describing the interactions among quarks and gluons. The fundamental color charges in this theory are confined in color-neutral objects known as baryons and mesons, containing three quarks and quark-antiquark pairs respectively. Since the advent of QCD, the existence of other, exotic, hadrons outside the conventional quark model, such as tetraquarks and pentaquarks, consisting of four or five valence quarks respectively, have been postulated, as early as in Murray Gell-Mann's introduction of the quark model [1].

Most exotic hadrons so far discovered contain at least one $c\bar{c}$ pair. The first proposed tetraquark candidate, the $X(3872)$, measured by Belle [2] in e^+e^- collisions, has been observed in many systems, including in nucleus-nucleus collisions [3]. The $Z(4430)$, a $c\bar{c}d\bar{u}$ tetraquark candidate was first measured by Belle [4] and later confirmed by LHCb [5]. The $Z(3900)$, reported by BES III [6] and Belle [7], was confirmed as a four-quark state. Most recently, LHCb announced the discovery of a $c\bar{c}c\bar{c}$ tetraquark, the $X(6900)$ [8]. LHCb has also announced the discovery of a $uudc\bar{c}$ pentaquark state, the $P_c(4312)^+$ [9]. So far no tetraquark states containing b quarks, either $q\bar{q}b\bar{b}$ or $b\bar{b}b\bar{b}$, have been confirmed.

The ANDY Collaboration has recently reported an observation of a resonance with a mass of 18.15 GeV in Cu+Au collisions at the Relativistic Heavy-Ion Collider (RHIC) [10]. This observation was made at forward rapidity and was interpreted as a $b\bar{b}b\bar{b}$ tetraquark state decaying to two $\Upsilon(1S)$ states, each decaying to hadrons through the $\Upsilon \rightarrow ggg$ channel. These data were taken at $\sqrt{s_{NN}} = 200$ GeV in 2012. They used a minimum bias trigger plus an inclusive jet and dijet trigger. Because no luminosity measurement was performed, the results were presented as fractions of the minimum bias yields.

In that analysis, multiple jets were found in a given event. Through an event-mixing study they found that only high energy dijets exhibited azimuthal angular correlations. No such correlations were observed for low energy dijets. They constructed the dijet mass for these large energy dijets and found peaks at $M_{\text{dijet}} = 17.83 \pm 0.2$ GeV for dijets with energy $250 < E < 260$ GeV and at $M_{\text{dijet}} = 18.47 \pm 0.22$ GeV for dijets with energy $260 < E < 270$ GeV. Both peaks have high statistical significance, 9σ and 8.4σ respectively, since there is little background in this region. Combining the two dijet energy bins gives an average dijet mass of $M_{\text{dijet}} = 18.12 \pm 0.15$ GeV. The two jets comprising the dijet were measured within the calorimeter acceptance $3.0 < \eta < 3.5$ [10]. They then looked for candidate $\Upsilon(1S)$ decays to three gluons and found evidence for double Υ production, both of which decayed hadronically through $\Upsilon(1S) \rightarrow 3g$. They concluded that the best candidate for their dijet mass signal is a $X_b(b\bar{b}b\bar{b})$ tetraquark state.

The authors of Ref. [10] noted that there have been many predictions of an X_b tetraquark mass, all of them larger than the ANDY value of 18.12 GeV. Karliner, Rosner and Nussinov [11] obtained a mass of 18.826 GeV based on meson and baryon mass systematics. A similar mass value, 18.84 ± 0.09 GeV, was found by Wang [12], based on QCD sum rules. Calculations of the ground state X_b mass by Bai, Lu and Osborne [13] and Wu *et al.* [14] found lighter masses of 18.69 GeV and 18.46 GeV respectively. Other calculations of $b\bar{b}b\bar{b}$ tetraquark states [15, 16] predict $\Upsilon(1S)\Upsilon(1S)$ tetraquark states with $J^{PC} = 1^{+-}$ with masses of ≈ 19 GeV, well above the ANDY mass but compatible

form a $\Lambda_c^+(udc)$ and $D^0(u\bar{c})$ from a $|uudc\bar{c}\rangle$ state or a final-state J/ψ with a proton. Leading charm asymmetries have been measured as a function of x_F and p_T in fixed-target $\pi^- + p$ interactions where a $D^-(d\bar{c})$, which can be produced from a $|\bar{u}dc\bar{c}\rangle$ Fock state of the negative pion, is leading over a $D^+(\bar{d}c)$ which is not [30]. It is worth noting that both D^+ and D^- can be produced at higher x_F than purely perturbative production in a higher Fock state, namely a six-particle $|\bar{u}ddd\bar{c}\bar{c}\rangle$ state, but there would be no difference in their distributions, neither would lead the other when produced from this state. In addition, the average x_F for D mesons hadronized from this state would be lower than the D^- average x_F from the minimal Fock state required to produce it, the four-particle $|\bar{u}dc\bar{c}\rangle$ state [31]. These higher Fock states would also have lower probabilities for manifestation from the projectile hadron.

In this work, the formulation for intrinsic heavy quarks in the proton wavefunction postulated by Brodsky and collaborators in Refs. [21, 22] has been adapted. That work was more specifically directed toward charm quarks. There are also other variants of intrinsic charm distributions in the proton, including meson-cloud models where the proton fluctuates into a $\bar{D}(u\bar{c})\Lambda_c(udc)$ state [33–36], also resulting in forward production, or a sea-like distribution [37, 38], only enhancing the distributions produced by massless parton splitting functions as in DGLAP evolution. Intrinsic charm has also been included in global analyses of the parton densities [37–41]. (See Ref. [42] for a discussion of a possible kinematic constraint on intrinsic charm in deep-inelastic scattering.)

The probability of intrinsic charm production, P_{ic5}^0 , obtained from these analyses, as well as others, has been suggested to be between 0.1% and 1%. The reviews in Refs. [43, 44] describe the global analyses and other applications of intrinsic heavy quark states. New evidence for a finite charm quark asymmetry in the nucleon wavefunction from lattice gauge theory, consistent with intrinsic charm, was presented in Ref. [45].

The general consensus is that the probability of intrinsic bottom production, P_{ib5}^0 , will scale as the square of the quark mass, m_c^2/m_b^2 , for production from a minimal Fock state configuration such as $|uudQ\bar{Q}\rangle$ where $Q = c, b$. A few calculations of intrinsic bottom production have been made previously [46, 47]. Some additional prior results are also summarized in Ref. [43].

Here single Υ production from such a minimal Fock state configuration is summarized first with differences between results for charm and bottom highlighted. Starting from this baseline, single and double Υ production from the minimal Fock state configuration for Υ pair production, $|uud\bar{b}b\bar{b}\rangle$, is developed. The x_F and rapidity distributions are described and the Υ pair mass distributions are presented and the sensitivities of these distributions to calculational inputs are discussed. Some attention is paid to the normalized cross section for such states but the main focus of the discussion is whether the distributions produced in this approach are compatible with the kinematic range of the ANDY measurement and, if so, are the resulting mass distributions at all compatible with their measured mass.

A. Single Υ Production from a $|uud\bar{b}\rangle$ State

Production of a single Υ from a five-particle proton Fock state is considered first, analogous to J/ψ production from such a state, as recently studied in Ref. [48]. In the case of Υ production, the frame-independent probability distribution of a 5-particle $b\bar{b}$ Fock state in the proton is

$$dP_{ib5} = P_{ib5}^0 N_5 \int dx_1 \cdots dx_5 \int dk_{x1} \cdots dk_{x5} \int dk_{y1} \cdots dk_{y5} \frac{\delta(1 - \sum_{i=1}^5 x_i) \delta(\sum_{i=1}^5 k_{xi}) \delta(\sum_{i=1}^5 k_{yi})}{(m_p^2 - \sum_{i=1}^5 (m_{Ti}^2/x_i))^2}, \quad (1)$$

where $i = 1, 2, 3$ are the interchangeable light quarks (u, u, d) and $i = 4$ and 5 are the b and \bar{b} quarks respectively. Here N_5 normalizes the $|uud\bar{b}\rangle$ probability to unity and P_{ib5}^0 scales the unit-normalized probability to the assumed intrinsic bottom content of the proton. The delta functions conserve longitudinal (z) and transverse (x and y) momentum. The denominator of Eq. (1) is minimized when the heaviest constituents carry the largest fraction of the longitudinal momentum, $\langle x_b \rangle > \langle x_q \rangle$. Given that $m_Q \gg m_q$, one does not expect large differences between $\langle x_b \rangle$ and $\langle x_c \rangle$ from $|uud\bar{b}\rangle$ and $|uudc\bar{c}\rangle$ states respectively.

In Ref. [48], the J/ψ p_T distribution from intrinsic charm was calculated for the first time by integrating over the light and charm quark k_T ranges in Eq. (1). In that work, k_{Tq}^{\max} was set to 0.2 GeV while the default for k_{Tc}^{\max} was taken to be 1 GeV. The sensitivity of the results to the k_T integration range was tested by multiplying the maximum of the respective k_T ranges by 0.5 and 2 respectively.

In previous estimates of intrinsic bottom production where the mass distributions were not calculated, average values for the transverse masses of the constituent quarks, $m_{Ti}^2 = m_i^2 + k_{Ti}^2$, $m_{Tq} = 0.45$ GeV and $m_{Tb} = 4.6$ GeV were chosen [47]. The same procedure can be employed here for the Υ x_F distribution which is independent of the exact value of m_b chosen. Thus the x_F distribution can be calculated assuming simple coalescence of the b and \bar{b} in a single state, represented in Eq. (1) by the addition of a delta function, $\delta(x_F - x_4 - x_5)$, in the longitudinal direction, ignoring the k_T integrations where 4 and 5 represent the b and \bar{b} quarks. When the transverse directions are also

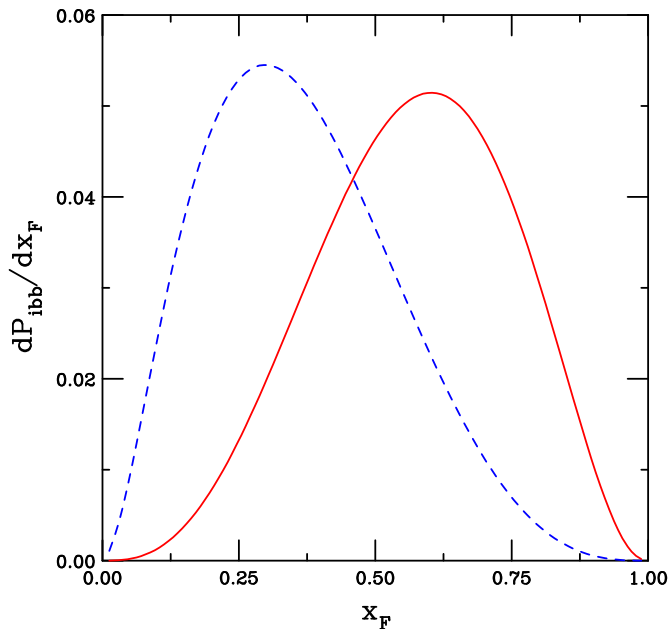


FIG. 1: (Color online) The probability distribution as a function of x for a single b quark (dashed blue curve) and as a function of x_F for a single Υ (solid red curve) from a five-particle Fock state of the proton. Both curves are normalized to unity.

included, employing $\delta(k_x \Upsilon - k_{x4} - k_{x5})$ and $\delta(k_y \Upsilon - k_{y4} - k_{y5})$, the x_F distribution is found to be independent of the k_T integration range.

Figure 1 shows the x distribution of a single b quark (dashed curve) and the x_F distribution of a single Υ (solid curve) from a five-particle proton Fock state. Such a calculation provides a check against previous results on the J/ψ . The average x of the b quark is 0.36 from a five-particle Fock state while the average x of a c quark is 0.34. Because the c and b quarks are both much more massive than the light quarks in the state, there is very little difference in the average longitudinal momentum carried by the heavy quarks.

The Υ x_F distribution has an average x_F of 0.57, somewhat less than twice the average x of the b quark. This average is 7.5% larger than the average x_F of the J/ψ from a similar five-particle proton Fock state. The x_F dependence is effectively independent of the chosen k_T limits, as shown in for single J/ψ production from a $|uudc\bar{c}\rangle$ state in Ref. [48].

Following the intrinsic charm cross section calculation in Ref. [48], the intrinsic bottom cross section from a $|uudb\bar{b}\rangle$ component of the proton can be written as

$$\sigma_{\text{ib}5}(pp) = P_{\text{ib}5}^0 \sigma_{pN}^{\text{in}} \frac{\mu^2}{4m_{Tb}^2}. \quad (2)$$

The factor of $\mu^2/4m_{Tb}^2$ arises from the soft interaction which breaks the coherence of the Fock state. The scale $\mu^2 = 0.1 \text{ GeV}^2$ is assumed for better agreement with the J/ψ A dependence, see Ref. [49]. An inelastic $p + N$ cross section of $\sigma_{pN}^{\text{in}} = 42 \text{ mb}$ is appropriate for RHIC energies.

The Υ cross section can be obtained from Eq. (2) analogously to how the cross section is obtained in perturbative QCD using the color evaporation model (CEM) which relates the $Q\bar{Q}$ cross section to the quarkonium cross sections. The same factor, $F_B = 0.022$, determined from recent CEM calculations [50] for inclusive prompt Υ production, is used here to relate the intrinsic bottom cross section to the Υ cross section from the same state,

$$\sigma_{\text{ib}5}^{\Upsilon}(pp) = F_B \sigma_{\text{ib}5}(pp). \quad (3)$$

The nuclear dependence of the intrinsic bottom contribution is assumed to be the same as that extracted for the nuclear surface-like component of J/ψ dependence by the NA3 Collaboration [51],

$$\sigma_{\text{ib}5}^{\Upsilon}(pA) = \sigma_{\text{ib}5}^{\Upsilon}(pp) A^{\beta} \quad (4)$$

with $\beta = 0.71$ [51] for a proton beam. In that experiment, two contributions to the cross section were separated, a volume-type component, with a close-to-linear nuclear dependence, and the diffractive component, associated with

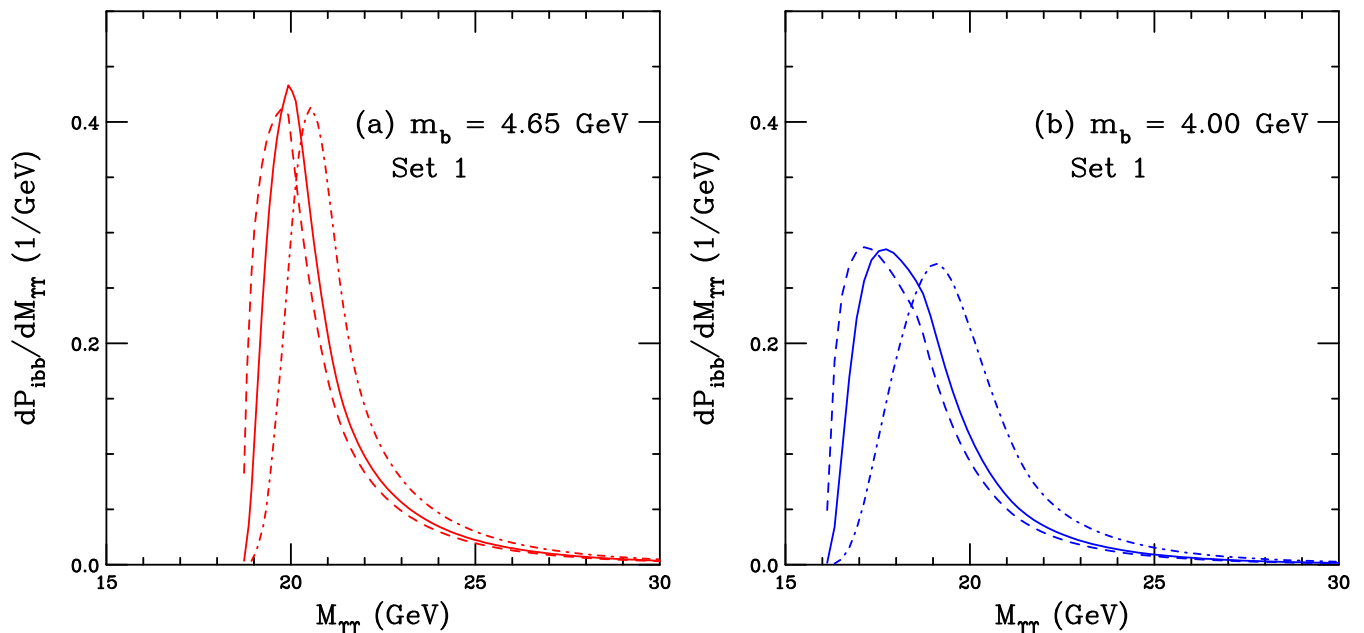


FIG. 3: (Color online) The probability for double Υ production from a seven-particle Fock state as a function of the pair mass for three different k_T integration ranges, corresponding to Set 1 in Table I, are shown: $k_q^{\max} = 0.2$ GeV, $k_b^{\max} = 1.0$ GeV and $k_\Upsilon^{\max} = 1.0$ GeV (solid); $k_q^{\max} = 0.1$ GeV, $k_b^{\max} = 0.5$ GeV and $k_\Upsilon^{\max} = 0.5$ GeV (dashed); and $k_q^{\max} = 0.4$ GeV, $k_b^{\max} = 2.0$ GeV and $k_\Upsilon^{\max} = 2.0$ GeV (dot-dashed). All distributions are normalized to unity. In (a) $m_b = 4.65$ GeV while in (b) $m_b = 4.00$ GeV.

the x and k_T of the pair itself. The delta functions insure conservation of momentum for both Υ mesons and the $\Upsilon\Upsilon$ pair.

Figure 3 shows the predictions for the $\Upsilon\Upsilon$ pair mass distributions. All distributions are normalized to unity. Without any k_T dependence, the pair mass distribution is strongly peaked at the $4m_b$ threshold. The k_T dependence smears out the pair distribution, increasing $\langle M_{\Upsilon\Upsilon} \rangle$ by several GeV. The chosen default values of the transverse momentum range, $k_q^{\max} = 0.2$ GeV and $k_b^{\max} = 1.0$ GeV, as also assumed for light quarks and charm quarks respectively in a five-particle proton Fock state for J/ψ production [48]. In addition, the k_Υ integration range also is required to calculate the Υ pair mass distribution. The value $k_\Upsilon^{\max} = 1$ GeV is used as a default for both the Υ k_T range as well as that for the Υ pair. The pair mass distributions for $m_b = 4.65$ GeV, the bottom quark mass used in bottom quark calculations at next-to-leading order [24], are shown in the solid curve of Fig. 3(a).

The mass threshold is well above the average Υ pair mass of 18.15 GeV reported by the ANDY Collaboration [10]. The average pair mass in all cases is greater than 20 GeV. Varying the transverse integration range by increasing (dot-dashed curve) or decreasing (dashed curve) the range by a factor of two does not change the mass threshold and alters the average pair mass by less than 0.5 GeV, see the results labeled Set 1 on the left-hand side of Table I.

The pair mass obtained with the 1S value of m_b is much higher than the ANDY result. The lower value of the bottom quark mass, 4 GeV, used with the same set of transverse momentum integration ranges, does result in a lower average mass, as shown in Fig. 3(b). Even though the threshold is reduced and the average pair mass is decreased to ≈ 19 GeV, see the upper results on the right-hand side of Table I, these values are still higher than obtained by the ANDY Collaboration.

In Ref. [27], predictions for double Υ production from the seven-particle Fock state were given assuming $m_{Tb} = 4.6$ GeV. (In that work, only averages were reported, no distributions were presented, and no systematic studies of the mass and transverse momentum were carried out.) It was found that the single Υ and $\Upsilon\Upsilon$ pair x distributions were similar to the equivalent $J/\psi J/\psi$ distributions. The average mass, $\langle M_{\Upsilon\Upsilon} \rangle$, was found to be 21.7 GeV for a proton beam, a few GeV above the two Υ mass threshold, $2m_\Upsilon = 18.9$ GeV. These results are in good agreement with the central value obtained for $m_b = 4.65$ GeV shown in Fig. 3(a) and in Table I.

The Υ pair mass distributions are quite sensitive to the range of k_T integration. Results for other values of k_q^{\max} , k_b^{\max} and k_Υ^{\max} are shown for both values of m_b considered. Sets 2 through 5 in Table I give the average Υ pair mass for each central value as well as for halving and doubling the ranges for each chosen central value. Note that the central value of k_q^{\max} is always 0.2 GeV. The central value of k_b^{\max} is varied from 1 to 2 GeV and, finally, the central value of k_Υ^{\max} is either 1, 2 or 5 GeV. The value of k_b^{\max} is assumed to be either less than or equal to k_Υ^{\max} , never

Set	$m_b = 4.65$ GeV				$m_b = 4.00$ GeV			
	k_q^{\max} (GeV)	k_b^{\max} (GeV)	k_Υ^{\max} (GeV)	$\langle M_{\Upsilon\Upsilon} \rangle$ (GeV)	k_q^{\max} (GeV)	k_b^{\max} (GeV)	k_Υ^{\max} (GeV)	$\langle M_{\Upsilon\Upsilon} \rangle$ (GeV)
1	0.2	1.0	1.0	21.02	0.2	1.0	1.0	18.96
	0.1	0.5	0.5	20.74	0.1	0.5	0.5	18.59
	0.4	2.0	2.0	21.60	0.4	2.0	2.0	19.98
2	0.2	1.0	2.0	21.37	0.2	1.0	2.0	19.47
	0.1	0.5	1.0	20.87	0.1	0.5	1.0	18.76
	0.4	2.0	4.0	22.12	0.4	2.0	4.0	20.82
3	0.2	2.0	2.0	21.59	0.2	2.0	2.0	19.98
	0.1	1.0	1.0	21.02	0.1	1.0	1.0	18.95
	0.4	4.0	4.0	22.56	0.4	4.0	4.0	21.33
4	0.2	1.0	5.0	22.10	0.2	1.0	5.0	21.01
	0.1	0.5	2.5	21.49	0.1	0.5	2.5	19.62
	0.4	2.0	10.0	22.68	0.4	2.0	10.0	22.04
5	0.2	2.0	5.0	22.32	0.2	2.0	5.0	21.17
	0.1	1.0	2.5	21.56	0.1	1.0	2.5	19.77
	0.4	4.0	10.0	23.88	0.4	4.0	10.0	22.98

TABLE I: The average Υ pair mass for given values of the bottom quark mass and the maximum range of k_T integration for light quarks, bottom quarks, and the Υ state.

larger.

The larger the upper limit of the range of integration over momentum, the larger the average pair mass becomes. The bottom quark mass obtained from the $\Upsilon(1S)$, $m_b = 4.65$ GeV, gives a consistently higher mass of the double Υ state, always greater than 20 GeV. On the other hand, the lower limit chosen for the b quark mass, 4 GeV, results in a smaller Υ pair mass, as low as 18.6 GeV, but still larger than the average Υ pair mass reported by ANDY.

The pair mass distributions are shown in Figs. 4 and 5 from Sets 2-5 of k_T integration ranges in Table I. The central values, the first line of each set in the table, are shown by the solid curves while the dashed curve shows the result for the integration range reduced by half and the dot-dashed curve presents the results for doubling the k_T integration range. All distributions are normalized to unity. It is clear that not just the average pair mass increases with the integration range in k_T but also the width of the distribution. In cases where half the integration range is taken (dashed curves), the width is narrower while, when the integration range is doubled (dot-dashed curves), the distributions are broader.

None of the results presented here are compatible with the ANDY results. Indeed, increasing the integration range does not affect the threshold and effectively only serves to increase the pair mass. Unlike the earlier NA3 results on double J/ψ production, where the pair mass was well above twice the J/ψ mass, the ANDY Collaboration reports an average pair mass *below* twice the mass of a single $\Upsilon(1S)$ state, 18.92 GeV. Assuming $m_b = 4$ GeV in the $b\bar{b}$ pair mass integration, it is possible to obtain a pair mass below $2m_\Upsilon$ but this seems unlikely, especially since it is obtained with a particularly low bottom quark mass, less than what is generally assumed for the current bottom quark mass. Indeed, in calculations of uncertainty bands on perturbative bottom quark production such as in FONLL [55], the b quark mass range is $4.5 \leq m_b \leq 5$ GeV.

It is noteworthy, however, that the average calculated pair masses, for Set 1 and $m_b = 4$ GeV, as in Fig. 3(b), are relatively compatible with the models of X_b masses. The next section considers the effects on the distributions reported here if the internal kinematics of the Fock state assumes a single tetraquark configuration of $b\bar{b}b\bar{b}$ not directly bound in an Υ pair.

C. X_b Tetraquark Production from a $|uud\bar{b}\bar{b}\bar{b}\bar{b}\rangle$ State

The restriction of two $\Upsilon(1S)$ states produced from the $|uud\bar{b}\bar{b}\bar{b}\bar{b}\rangle$ Fock state is lifted in this section to determine whether a direct X_b configuration, without the assumption of two bound $\Upsilon(1S)$ states, might be more compatible with the reported ANDY mass distribution.

The same starting point, Eq. (7), is assumed. Now, however, the x_F distribution is calculated with the addition of a single longitudinal delta function, $\delta(x_{X_b} - x_4 - x_5 - x_6 - x_7)$. Despite the rearrangement of the bottom quarks

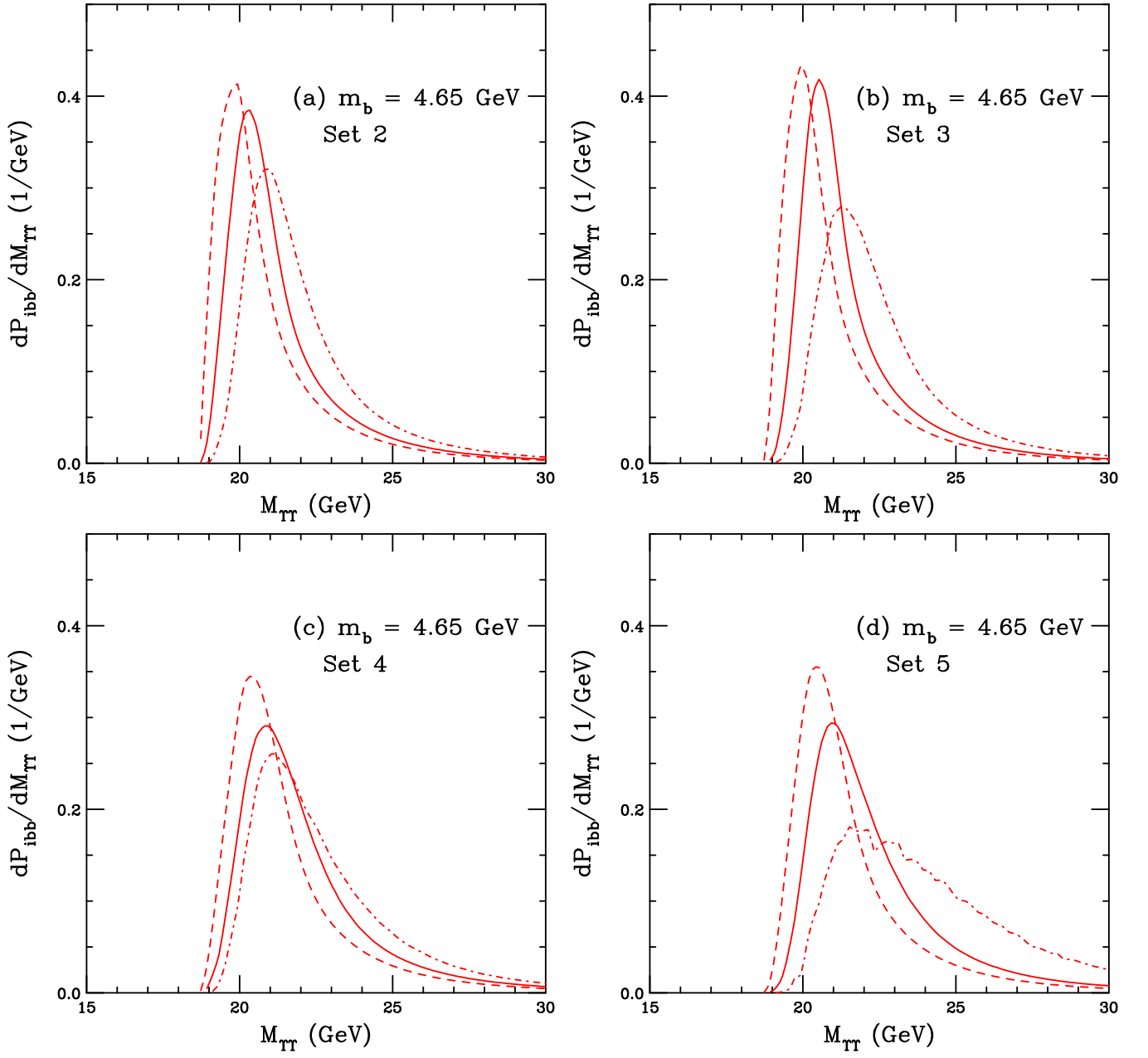


FIG. 4: (Color online) The double Υ pair mass distribution normalized to unity from a seven-particle proton Fock state with $m_b = 4.65$ GeV. Different k_T integration ranges, corresponding to Sets 2-5 of Table I, are shown in (a)-(d) respectively. In each case, the solid curve shows the calculation for the central value of the range while the dashed and dot-dashed curves show half and double the central value of the ranges respectively.

in this configuration, the $M_{X_b} x_F$ distribution is identical to the one for the Υ pair shown in the dashed curve in Fig. 2(a). This suggests that the longitudinal distributions are independent of any correlations between the partons in the state as long as the same number and type of partons are included.

Next, the mass distributions are calculated, without including the pair mass constraints, $2m_b < m_{T\Upsilon} < 2m_B$, in Eq. (12). The X_b mass distribution is then

$$\begin{aligned} \frac{dP_{\text{ibb}7}}{dM_{X_b}^2} &= \int \frac{dx_{X_b}}{x_{X_b}} \int dk_{x_{X_b}} dk_{y_{X_b}} dP_{\text{ibb}7} \delta\left(\frac{M_{T,X_b}^2}{x_{X_b}} - \frac{m_{T,4}^2}{x_4} - \frac{m_{T,5}^2}{x_5} - \frac{m_{T,6}^2}{x_6} - \frac{m_{T,7}^2}{x_7}\right) \\ &\times \delta(k_{x_4} + k_{x_5} + k_{x_6} + k_{x_7} - k_{x_{X_b}}) \delta(k_{y_4} + k_{y_5} + k_{y_6} + k_{y_7} - k_{y_{X_b}}) \delta(x_{X_b} - x_4 - x_5 - x_6 - x_7), \end{aligned} \quad (13)$$

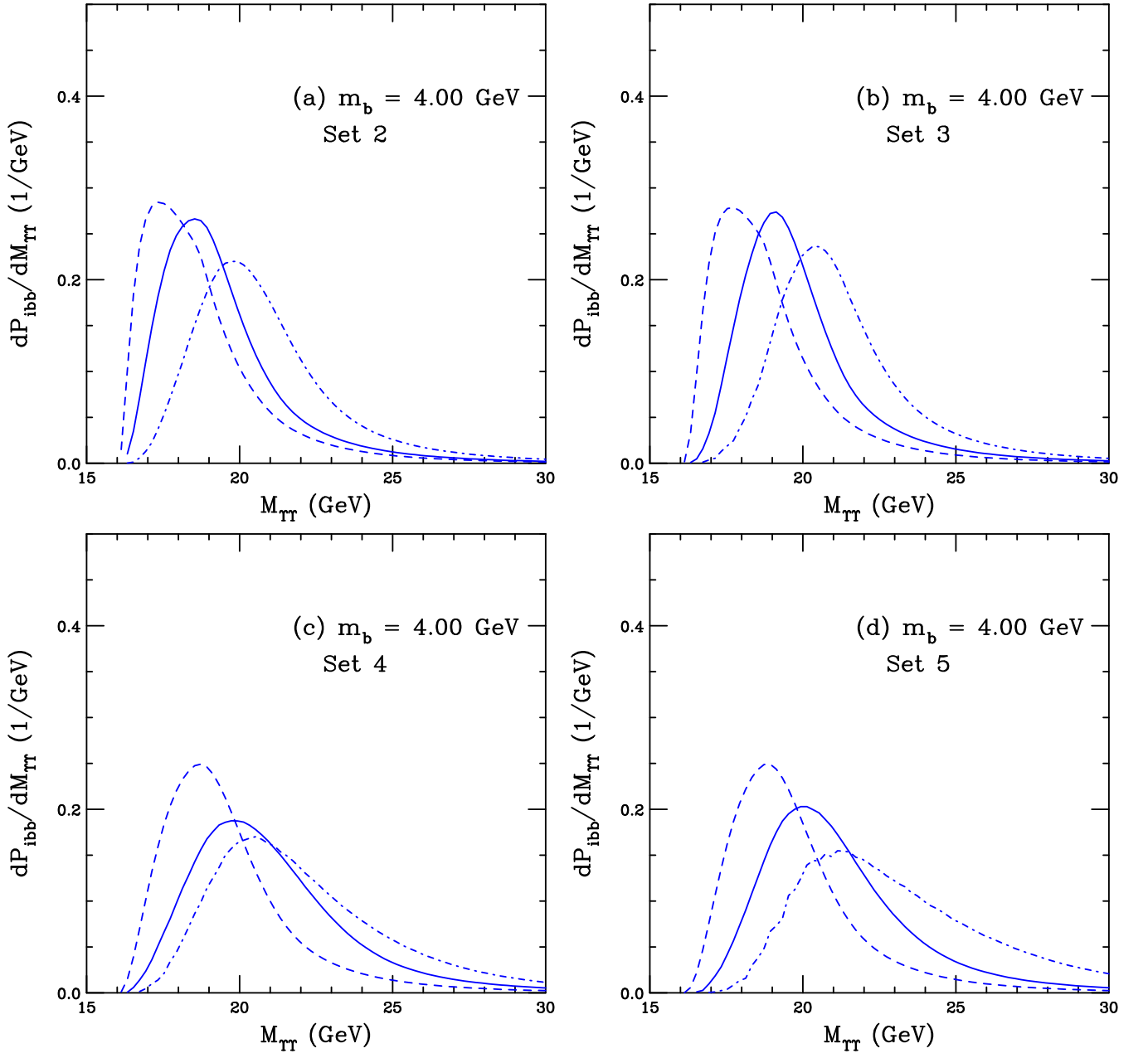


FIG. 5: (Color online) The double Υ pair mass distribution normalized to unity from a seven-particle proton Fock state with $m_b = 4.00$ GeV. Different k_T integration ranges, corresponding to Sets 2-5 of Table I, are shown in (a)-(d) respectively. In each case, the solid curve shows the calculation for the central value of the range while the dashed and dot-dashed curves show half and double the central value of the ranges respectively.

where dP_{ibb7} is from Eq. (7).

The mass distributions for the X_b from Eq. (13) are shown in Fig. 6 for the same values of m_b , k_q^{\max} and k_b^{\max} as shown in Fig. 3 (Set 1 in Table II). In this case the k_T range for the X_b is taken to be the same as for the b quarks. The results here are also normalized to unity.

The mass distributions are much broader than those in Fig. 3, even though they have the same thresholds. They become broader because there is no integration over the Υ mass in this case, as in Eq. (12), where the Υ mass was restricted to be between $2m_b$ and $2m_B$. These broader distributions result in higher average masses for the X_b , typically 1-2 GeV higher than for the same Fock state where the $b\bar{b}b\bar{b}$ is considered to be bound into an Υ pair. Thus, no further systematic studies of the mass dependence on k^{\max} are considered here. The average X_b masses from these

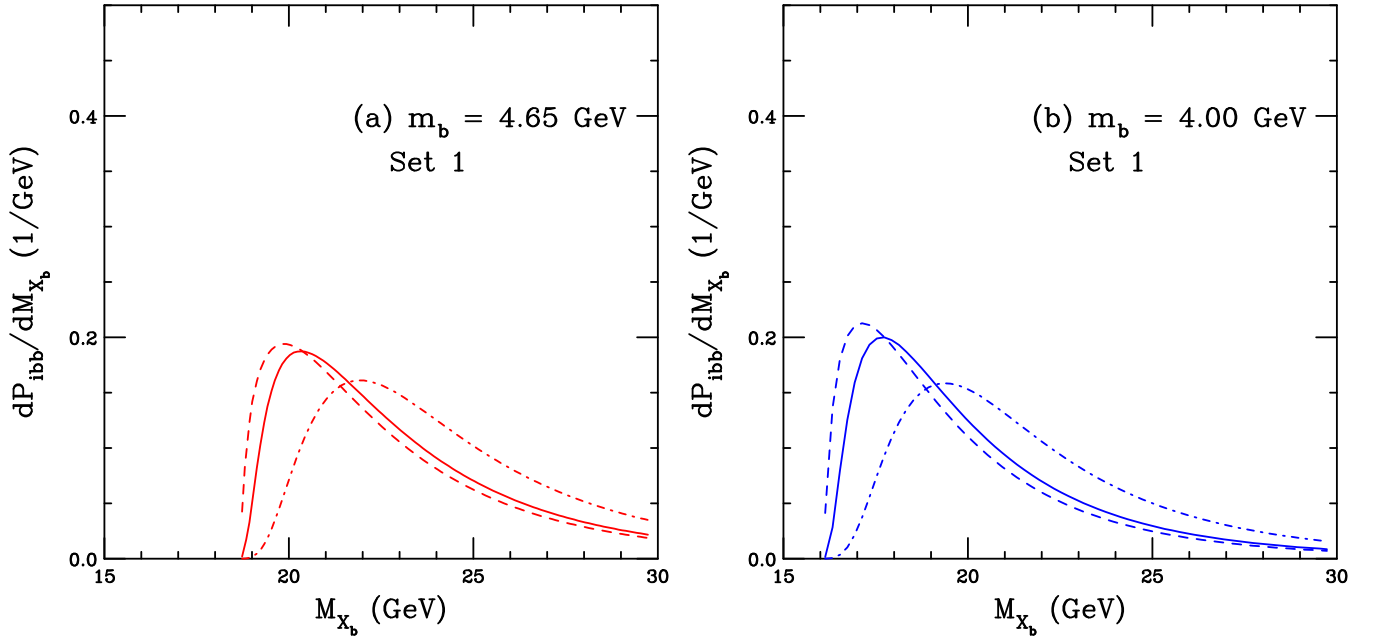


FIG. 6: (Color online) The probability for X_b production from a seven-particle Fock state as a function of the X_b mass for three different k_T integration ranges, corresponding to Set 1 in Table II, are shown: $k_q^{\max} = 0.2$ GeV, different k_T integration ranges are shown: $k_q^{\max} = 0.2$ GeV, $k_b^{\max} = 1.0$ GeV and $k_{X_b}^{\max} = 1.0$ GeV (solid); $k_q^{\max} = 0.1$ GeV, $k_b^{\max} = 0.5$ GeV and $k_{X_b}^{\max} = 0.5$ GeV (dashed); and $k_q^{\max} = 0.4$ GeV, $k_b^{\max} = 2.0$ GeV and $k_{X_b}^{\max} = 2.0$ GeV (dot-dashed). All distributions are normalized to unity. In (a) $m_b = 4.65$ GeV while in (b) $m_b = 4.0$ GeV.

Set	$m_b = 4.65$ GeV				$m_b = 4.00$ GeV			
	k_q^{\max} (GeV)	k_b^{\max} (GeV)	$k_{X_b}^{\max}$ (GeV)	$\langle M_{X_b} \rangle$ (GeV)	k_q^{\max} (GeV)	k_b^{\max} (GeV)	$k_{X_b}^{\max}$ (GeV)	$\langle M_{X_b} \rangle$ (GeV)
1	0.2	1.0	1.0	22.66	0.2	1.0	1.0	20.11
	0.1	0.5	0.5	22.31	0.1	0.5	0.5	19.65
	0.4	2.0	2.0	23.72	0.4	2.0	2.0	21.47

TABLE II: The average X_b mass for given values of the bottom quark mass and the maximum range of k_T integration for light quarks, bottom quarks, and the X_b .

calculations are given in Table II, corresponding to the first three rows of Table I.

It is worth noting that the probability for an X_b state could be considerably different from that of a double Υ state. The factors of F_B for Υ production, as in Eq. (9), would be replaced by a single factor F_{X_b} , giving

$$\sigma_{\text{ibb}7}^{X_b}(pp) = F_{X_b} \frac{P_{\text{ibb}7}^0}{P_{\text{ib}5}^0} \sigma_{\text{ib}5}(pp). \quad (14)$$

In the CEM, F_B is determined by a fit to Υ production data. Since no all bottom tetraquark states have so far been reported, aside from the ANDY result which did not determine a cross section, the extraction of F_{X_b} is not yet possible.

Finally, one could consider a tetraquark to be produced as a single massive object rather than composed of two individual $b\bar{b}$ pairs. In such a case, the tetraquark could be assumed to be produced in a four-particle Fock state, $|uudX_b\rangle$, similar to a massive gluon. However, this configuration does not have a mass threshold and would carry a lower share of the nucleon momentum on average, $\langle x_{X_b} \rangle \sim 0.5$ as long as $\hat{M}_{X_b} \gg \hat{m}_q$. Thus this type of state would not conform to the kinematic criteria required for either a double Υ state or an $X_b(b\bar{b}b\bar{b})$ state.

- 311 (1996).
- [31] T. Gutierrez and R. Vogt, Leading charm in hadron nucleus interactions in the intrinsic charm model, Nucl. Phys. B **539**, 189 (1999).
 - [32] S. J. Brodsky, P. Hoyer, A. H. Mueller, and W.-K. Tang, New QCD production mechanisms for hard processes at large x , Nucl. Phys. B **369**, 519 (1992).
 - [33] S. Paiva, M. Nielsen, F. S. Navarra, F. O. Duraes and L. L. Barz, Virtual meson cloud of the nucleon and intrinsic strangeness and charm, Mod. Phys. Lett. A **13**, 2715 (1998).
 - [34] M. Neubert, Heavy quark symmetry, Phys. Rept. **245**, 259 (1994).
 - [35] F. M. Steffens, W. Melnitchouk, and A. W. Thomas, Charm in the nucleon, Eur. Phys. J. C **11**, 673 (1999).
 - [36] T. J. Hobbs, J. T. Londergan and W. Melnitchouk, Phenomenology of nonperturbative charm in the nucleon, Phys. Rev. D **89**, 074008 (2014).
 - [37] J. Pumplin, H. L. Lai, and W. K. Tung, The Charm Parton Content of the Nucleon, Phys. Rev. D **75**, 054029 (2007).
 - [38] P. M. Nadolsky *et al.*, Implications of CTEQ global analysis for collider observables, Phys. Rev. D **78**, 013004 (2008).
 - [39] S. Dulat *et al.*, Intrinsic Charm Parton Distribution Functions from CTEQ-TEA Global Analysis, Phys. Rev. D **89**, 073004 (2014).
 - [40] P. Jimenez-Delgado, T. J. Hobbs, J. T. Londergan and W. Melnitchouk, New limits on intrinsic charm in the nucleon from global analysis of parton distributions, Phys. Rev. Lett. **114**, 082002 (2015).
 - [41] R. D. Ball *et al.* [NNPDF Collaboration], A Determination of the Charm Content of the Proton, Eur. Phys. J. C **76**, 647 (2016).
 - [42] J. Blumlein, A kinematic condition on intrinsic charm, Phys. Lett. B **753**, 619 (2016).
 - [43] S. J. Brodsky, A. Kusina, F. Lyonnet, I. Schienbein, H. Spiesberger, and R. Vogt, A review of the intrinsic heavy quark content of the nucleon, Adv. High Energy Phys. **2015**, 341547 (2015).
 - [44] S. J. Brodsky, G. I. Lykasov, A. V. Lipatov and J. Smiesko, Novel Heavy-Quark Physics Phenomena, Prog. Part. Nucl. Phys. **114**, 103802 (2020).
 - [45] R. S. Sufian, T. Liu, A. Alexandru, S. J. Brodsky, G. F. de Téramond, H. G. Dosch, T. Draper, K. F. Liu and Y. B. Yang, Constraints on charm-anticharm asymmetry in the nucleon from lattice QCD, Phys. Lett. B **808**, 135633 (2020).
 - [46] E. Norrbin and R. Vogt, Bottom production asymmetries at the LHC, [arXiv:hep-ph/0003056 [hep-ph]].
 - [47] R. Vogt and S. J. Brodsky, QCD and intrinsic heavy quark predictions for leading charm and beauty hadroproduction, Nucl. Phys. B **438**, 261 (1995).
 - [48] R. Vogt, Limits on Intrinsic Charm Production from the SeaQuest Experiment, Phys. Rev. C **103**, 035204 (2021).
 - [49] R. Vogt, S.J. Brodsky, and P. Hoyer, Systematics of J/ψ Production, Nucl. Phys. B **360**, 67 (1991).
 - [50] R. Vogt, Shadowing effects on J/ψ and Υ production at energies available at the CERN Large Hadron Collider, Phys. Rev. C **92**, 034909 (2015).
 - [51] J. Badier *et al.* [NA3 Collaboration], Experimental J/ψ Hadronic Production from 150 GeV/ c to 280 GeV/ c , Z. Phys. C **20**, 101 (1983).
 - [52] R. E. Nelson, R. Vogt, and A. D. Frawley, Narrowing the Uncertainty on the Total Charm Cross Section and its Effect on the J/ψ Cross Section, Phys. Rev. C **87**, 014908 (2013).
 - [53] P. A. Zyla *et al.* (Particle Data Group), The Review of Particle Physics (2021), Prog. Theor. Exp. Phys. 2020, 083C01 (2020) and 2021 update.
 - [54] R. Vogt, Heavy Flavor Azimuthal Correlations in Cold Nuclear Matter, Phys. Rev. C **98**, 034907 (2018).
 - [55] M. Cacciari, P. Nason and R. Vogt, QCD predictions for charm and bottom production at RHIC, Phys. Rev. Lett. **95**, 122001 (2005).